Journal of Aerosol Science 64 (2013) 11–23

Contents lists available at SciVerse ScienceDirect

Journal of Aerosol Science

journal homepage: www.elsevier.com/locate/jaerosci

Retrieving the relative contribution of aerosol types from single particle analysis and radiation measurements and calculations: A comparison of two independent approaches

Mariana Achad [a], María Laura López [b], Gustavo G. Palancar [a], Beatriz M. Toselli [a,*]

[a] Departamento de Físico Química/INFIQC/CONICET/CLCM, Facultad de Ciencias Químicas, Universidad Nacional de Córdoba, Ciudad Universitaria, Pabellón Argentina, 5000 Córdoba, Argentina
[b] Facultad de Matemática, Astronomía y Física/IFEG/CONICET, Universidad Nacional de Córdoba, Ciudad Universitaria, 5000 Córdoba, Argentina

ARTICLE INFO

Article history:
Received 26 March 2013
Received in revised form
30 May 2013
Accepted 31 May 2013
Available online 18 June 2013

Keywords:
Aerosol types
Single particle analysis
SEM-EDX
SBDART model
UV-B irradiance
Aerosol optical properties

ABSTRACT

The main purpose of this work is to determine the relative contribution of different types of aerosols at an urban site by using two independent approaches: individual particle analysis, and radiative transfer calculations and irradiance measurements. To accomplish that purpose, we used our UV-B irradiance (280–315 nm) data set, the AERONET (AErosol RObotic NETwork) database, the SEM (Scanning Electron Microscopy, LEO 1450VP) analyses of the collected particles and the Santa Barbara DISORT Atmospheric Radiative Transfer (SBDART) model. On one hand, the collected particles were analyzed by SEM-EDX (Energy Dispersive X-Ray, Genesis 2000) in order to determine their chemical composition. Then, by using a developed algorithm they were classified as rural or urban, resulting in a $(24 \pm 3)\%$ of rural and $(76 \pm 8)\%$ of urban. On the other hand, aerosols were incorporated into the SBDART model through two of its default profiles (urban or rural) and by using the Aerosol Optical Depth (AOD) provided by AERONET. The aerosol effect on experimental surface UV-B irradiance was reproduced by a linear combination of the irradiances calculated by using these profiles. From this analysis we found that, in average, a mix of aerosols of $(30 \pm 3)\%$ rural and $(70 \pm 7)\%$ urban explains the observed reduction in the experimental irradiance. Considering the agreement between the results obtained by using these two independent methodologies, the use of the irradiance as a surrogate variable to retrieve aerosol types is discussed. The methodology presented here is applicable to any site provided irradiance measurements and AOD are available.

1. Introduction

The importance of aerosols has been increasingly stressed in the recent decades. Many studies have looked at their influence on climate trough their contribution to radiative forcing. As aerosols scatter and absorb solar radiation, changes in their atmospheric concentrations and their chemical and physical properties can alter the transmission of the radiation through the atmosphere. That is why they are considered drivers of the climate change (Intergovernmental Panel on Climate Change (IPCC), 2007). Regardless of the large number of studies dealing with the radiative properties of aerosols, their net effect on global climate is still unknown and represents one of the major uncertainties in the understanding of Earth's climate system (Bond & Bergstrom, 2006). On other hand, aerosols with aerodynamic diameter less than 10 (PM10) and 2.5

* Corresponding author. Tel.: +54 351 4334169; fax: +54 351 4334188.
E-mail addresses: tosellib@fcq.unc.edu.ar, tosellib@yahoo.com.ar (B.M. Toselli).

0021-8502/$ - see front matter © 2013 Elsevier Ltd. All rights reserved.
http://dx.doi.org/10.1016/j.jaerosci.2013.05.008

(PM2.5) μm are considered among the main pollutants of concern, especially in urbanized areas, where they have been directly related with the incidence and severity of respiratory diseases (Dockery, 2009).

Particulate matter comprises a huge number of species with heterogeneous morphology and chemical composition, which leads to different optical properties. In order to deal with this complexity different methods, techniques, and approaches are used.

To study the chemical composition of aerosol samples, two approaches can be considered: bulk analysis and individual particles analysis (e.g. Moroni et al., 2012; Rashki et al., 2013). While bulk analysis provides the average composition of the sample, the analysis of the individual particles, using techniques such as Transmission Electron Microscopy (TEM), Scanning Electron Microscopy (SEM) and Electron Probe X-Ray Microanalysis (EPMA) coupled with Energy Dispersive X-Ray Analysis (EDX), provides more detailed information (e.g. Laskin, 2010). These techniques have been used to analyze the composition of particles which are present in different environments (e.g. outdoor air in Buenos Aires City (Bogo et al., 2003), indoor air affected by tobacco smoke (Slezakova et al., 2011), and Mexico City subway system (Mugica-Álvarez et al., 2012)). Once the chemical composition has been obtained, different algorithms (e.g. Ro et al., 2001; Willis et al., 2002) and the previous knowledge of the site (López et al., 2011) can be used to classify the particles according to the abundance of the elements present in the samples.

To retrieve or infer the optical properties of aerosols different procedures, based on the interaction between particles and radiation, are extensively used (e.g. Giles et al., 2012). The two main approaches are experimental measurements and model calculations. Radiation measurements can be made at the surface (Srivastava et al., 2012) or from different platforms such as tethered balloons (de Roode et al., 2001), hang-gliders (Junkermann, 1994), stratospheric balloons (Madronich et al., 1985), fixed-wing aircraft (Palancar et al., 2011), and satellites (Kaskaoutis et al., 2011). Aerosol optical properties retrieved from satellites are usually validated against surface measurements (Estellés et al., 2012; Aaltonen et al., 2012). On the other hand, radiative transfer models allow including the aerosols properties, measured or supposed for a hypothetical situation, in order to study their effects on radiation. For example, Sinha et al. (2013) have used the Santa Barbara DISORT Atmospheric Radiative Transfer (SBDART) model to calculate the aerosol radiative forcing. Andrada et al. (2008) used the Tropospheric Ultraviolet and Visible (TUV) model to simulate the UV-B irradiance in the presence of aerosols and compare it with measurements at the surface.

Although there are several works that have studied the aerosols chemical composition and others that have analyzed their optical properties, it would be interesting to have a way to relate these two pieces of information. Some authors have already made one step towards this objective. For example, Andreae et al. (2008) related the results obtained for single scattering albedo with chemical composition, Che et al. (2009) studied the spatial and temporal characteristics of aerosol optical depth and Ångström wavelength exponent and their relationship with aerosol chemical composition and morphology, Dumka et al. (2011) studied the altitude profile of spectral aerosol optical depths, mass concentration of aerosol black carbon, and total concentration of composite aerosols measured at several altitude levels, and Titos et al. (2012) have investigated the optical properties, the mass concentration, and the chemical composition of the aerosols at an urban site in Spain.

In Córdoba there are only a few studies regarding to aerosol characterization. In one of these studies, in an air quality campaign carried out by the City government in the period 1995–2001, PM10 concentration was measured and it was the only pollutant that has exceeded several times the 24 h national standard of 150 $\mu g\, m^{-3}$ (Olcese and Toselli, 1997). Unfortunately, the chemical composition of these samples was not determined. This is aggravated by the fact that no additional air quality monitoring is currently underway by any governmental agency. Recently, López et al. (2011) have carried out 24 h samplings of PM10 and PM2.5 during the period July 2009–April 2010 at an urban and at a semi-urban site of Córdoba City. The bulk chemical composition of aerosol particles was determined by Synchrotron Radiation X-Ray Fluorescence. Multivariate analysis of the elemental data resolved a number of components (sources) which, based on their chemical tracers, were assigned physical meanings. According to this study, mobile sources exhaust and pollution caused by traffic (urban resuspended dust) were responsible for 30% and 55% of the sources apportionment to PM2.5, respectively. Considering the scarcity of data in Córdoba, the present work has been performed in order to advance toward the knowledge of the aerosol characteristics and their radiative effects in the region.

The main purpose of this study was to determine the relative contribution of different types of aerosols at an urban site by using two independent approaches: individual particle analysis, and radiative transfer calculations and irradiance measurements. On one hand, SEM-EDX techniques were used to determine the chemical composition of the aerosol particles. A developed algorithm was then used to classify these particles as urban or rural types based on the chemical composition. On the other hand, the SBDART model was used to simulate the UV-B irradiance for aerosol loaded days. Aerosols were incorporated into the model by using two of its default aerosol profiles, urban or rural, and the optical depth provided by AERONET. The calculated irradiance resulting from a linear combination of these profiles was compared against experimental UV-B measurements in order to determine the contribution of each aerosol type. At the end, considerations to further correlate these two independent results are discussed.

2. Materials and methods

2.1. Study area and sampling site

The study was performed in Córdoba, the second largest city in Argentina with approximately 1.3 million inhabitants. It is located at latitude 31° 24′S and longitude 64°11′W, about 470 m a.s.l. The climate is sub-humid with a mean annual

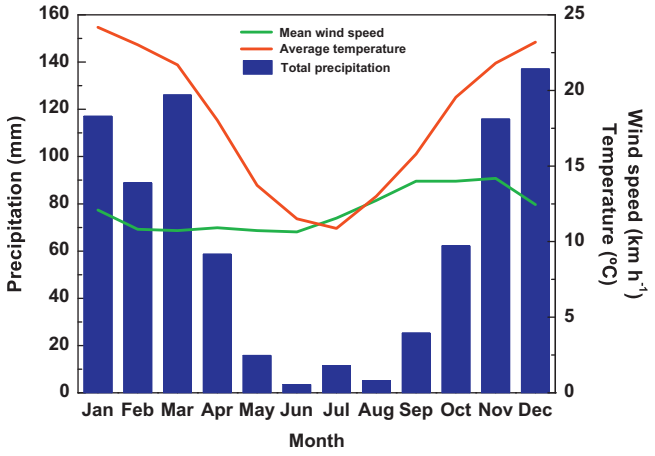

Fig. 1. Eleven year averages (2000–2010) of the mean wind speed, average temperature, and total precipitation for Córdoba. Data provided by the National Weather Service.

precipitation of 790 mm (concentrated mainly in summer time), a mean annual temperature of 17.4 °C and prevailing winds from NE (National Weather Service). The monthly variation of the mean wind speed, average temperature, and total precipitation for Córdoba is shown in Fig. 1, for an 11-year period (2000–2010). The soil is loessic and due to the presence of erosive agents it shows weak waves (Krohling, 1999). The west side of the city is surrounded by hills, which are subjected to fires, produced not only accidentally but also intentionally, especially during winter time. Fire plumes sometimes reach the city affecting the visibility and the air quality. In addition, a variety of industrial plants are located in the suburban areas surrounding the city, including automobile factories, auto-part industries, agro industries, and food processing companies. It is important to note that domestic heating is not an important factor at Córdoba City. The central area is densely built-up and is located in a depression. Most of the massive transport system runs 24 h (up to 700 units during the day) and crosses Córdoba downtown. Córdoba faces air pollution problems, especially during winter–spring time. This is because of the longer nights, the dry air, and the cloudless sky usually produce strong radiative inversions. As a consequence, pollutants and aerosols can be trapped in a layer lower than 200 m, in the morning hours, leading to adverse effects on health (Olcese & Toselli, 2002; Stein & Toselli, 1996).

Irradiance measurements and aerosol collection were carried out in a wide-open area in the university campus in Córdoba City. The site is southwest of downtown receiving the air pollution plume from the central area. The radiometers were placed on a cement yard surrounded by low buildings (that do not obstruct the air circulation), trees, grass, paved streets and bare soil. The impactor for the aerosol collection was placed at the balcony of the second floor of one of the buildings. This site is separated 150 m from a street that has a moderate flow of vehicles, close to 1000 vehicles per hour during daytime.

2.2. Aerosol collection, SEM-EDX analysis, and particle classification

All the aerosol samples were collected in the period of 2010–2011, during weekdays and with a sampling time between 3 h and 5 h. The samples were collected by using the Deployable Particulate Sampling system (DPS) with the SKC impactor to collect the PM2.5 fraction. The inertial impactor removed particles larger than a specific cut-point by capturing them on a disposable 37 mm pre-oiled porous plastic disk that reduces particle bounce. A flow rate of 10 L min^{-1} was maintained to ensure the maximum efficiency of the instrument. Particles were collected on cupper grids (Formvar®/Carbon 200 mesh, 30–50 nm thickness), a substrate which is known to be the most appropriate for single particle analysis (Laskin, 2010). After collecting the material, the grids were placed in polycarbonate petri dishes and stored in a desiccator until their analysis. The collection period covered a wide range of meteorological conditions.

All the particles were analyzed by SEM-EDX. SEM images of manually selected particles were recorded with a LEO 1450VP Scanning Electron Microscope using a combination of secondary and backscattered electrons. Semi-quantitative analysis was performed by using an Energy Dispersive X-ray Spectrometer (EDXS, Genesis 2000) and taking into consideration corrections for the ZAF effects related to atomic number (Z)-dependent electron scattering, absorption (A), and fluorescence (F) (Laskin, 2010; Willis et al., 2002). The magnifications ranged from 1000 up to 15000x. Prior to the analysis, the grids were mounted on an Al-stub using a conductive double-sided adhesive tape. No additional coating was necessary.

Given the huge variability in particle composition there are no standard algorithms that could be followed to classify unequivocally any set of sampled particles. In general, some common rules can be followed but they must be modified by adequate criteria, usually based on the knowledge of the site, meteorology, sources, previous studies, etc. (e.g. Chen et al., 2006; Hwang & Ro, 2006; Kang et al., 2009; Lorenzo et al., 2006). The single particle classification is usually based on the

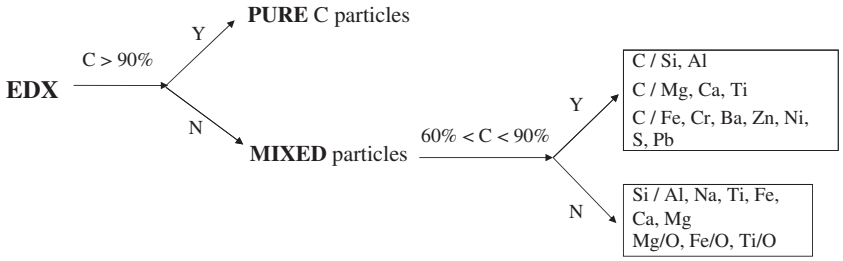

Fig. 2. Algorithm followed for the single particle classification.

intensity of the element signals (Willis et al., 2002) or on the weight percentage of the elements (e.g. Hwang & Ro, 2006; Kang et al., 2009). In this work, particles were first grouped based on the weight percentage (wt%) of the most abundant elements observed in the EDX spectra. Then, to classify them we developed the methodology shown in Fig. 2, which was based on the guidelines proposed in Ro et al. (2001) and on the knowledge of the meteorology and the sources which affect the study area (López et al., 2011; Olcese & Toselli, 1998). The main criterion for the classification of the particles was the wt% in C. First, particles with a wt% of at least 90% in this component were considered as pure particles. When more than one component was present, the particle was considered as a mixture of the most abundant ones. Thus, the second criterion was to group particles with a wt% in C between 60 and 90. For example, "C/Si, Al" denotes a particle which contains a mixture of carbon in a high percentage (wt%: 60–90) and silicon and aluminum as the second more abundant elements. Elements present in wt% lower than 5 were neglected. At the end, particles were grouped as urban or rural.

2.3. Solar irradiance measurements

Irradiance measurements have been carried out since 1999 by using a pyranometer YES (Yankee Environmental System, Inc.) model UVB-1 which measures UV-B (280–315 nm) global irradiance. The pyranometer was factory calibrated. The UVB-1 spectral response function has been given elsewhere (Palancar & Toselli, 2002, 2004). Details about uncertainties, calibration, and maintenance of the pyranometer can be found in Dichter et al. (1993), Bigelow et al. (1998), and López et al. (2012).

Observations were recorded as half a minute average values. Cloudless conditions were periodically assured by direct observers. Because visible and infrared wavelengths are more sensitive to cloud presence, the daily courses of total irradiance (300–3000 nm), measured with a YES model TSP-700 pyranometer, were used to double check the cloudless condition at all times. Additional meteorological data (ambient temperature, relative humidity, wind speed and direction, and precipitations) were provided by the National Weather Service.

2.4. SBDART model and irradiance calculations

SBDART model version 2.0 was used for all the calculations (Ricchiazi et al., 1998). They were carried out from 280 to 315 nm with a resolution of 1 nm. The surface albedo was assumed to be Lambertian, wavelength independent, and with a constant value of 0.05 throughout the year. Due to the low levels of tropospheric UV-B absorbing pollutants like O_3, SO_2, and NO_2 in Córdoba City (Olcese & Toselli, 2002), they were not considered in the calculations. Total ozone column values were obtained daily by the Total Ozone Mapping Spectrometer (TOMS) instrument onboard Earth Probe spacecraft (until 2005) and by the Ozone Monitoring Instrument (OMI) onboard Aura spacecraft (since 2006). Ozone data were provided by the Ozone Processing Team of the Goddard Space Flight Center of the National Aeronautic and Space Administration (NASA, United States). Mid latitude atmospheric profiles for summer and winter were considered. All the irradiance calculations were performed at solar zenith angles (SZA) smaller than 70°. For a more realistic calculation, the variability of AOD and relative humidity along the day was taken into account.

SBDART includes several models of lower atmosphere aerosols taken from the work of Shettle and Fenn (1979). Considering the geographic location of Córdoba, at the central region of Argentina, we assume that mainly two types of aerosols affect the city: urban and rural. Therefore, in our calculations we have only used these two default aerosol profiles. The differences between both profiles are based on how the aerosol optical properties, like extinction efficiency, asymmetry factor (g) and single scattering albedo (ω_o), vary with wavelength and to the extent the scattering parameters depend on the surface relative humidity (Ricchiazi et al., 1998). As guidance, the values at 300 nm and 0% relative humidity are, for the urban profile: $\omega_o = 0.639$, $g = 0.718$, and for the rural profile: $\omega_o = 0.932$, $g = 0.679$ (Shettle & Fenn, 1979). The aerosol optical depth (AOD) was taken from a nearby AERONET site. The AOD was measured with a CIMEL Electronique 318A Sun photometer at Córdoba-CETT station (31° 31′ S, 64° 27′ W, 730 m a.s.l.). Since 1999, this AERONET station provided measurements of AOD at seven spectral bands (340, 380, 440, 500, 670, 870 and 1020 nm). All AOD values used in this work were level 2.0. The station was operating until December 2010, when the Sun photometer was deployed at another region away from Córdoba. A detailed description of the instruments, data acquisition procedure, and calibration is given in Holben et al. (1998, 2001). An accuracy assessment of the AERONET retrievals can be found in the work of Dubovik et al. (2000).

Andrada et al. (2008) proved that the aerosols present in this AERONET site (about 20 km away from Córdoba city) have the same origin as those present in the site where the irradiance measurement were carried out, i.e. they have a regional character, and also that they are homogeneously mixed in the first kilometers of the troposphere.

As the AOD value at 550 nm (required by the model) is not provided by AERONET, the available AOD values for each day were adjusted to the Ångström's (1929) equation

$$AOD(\lambda) = \beta\lambda^{-\alpha} \tag{1}$$

where α and β are fitting parameters. The square correlation coefficients were always higher than 0.97. The AOD values at 550 nm ($AOD_{550\ nm}$) for each day and time of interest were found evaluating the corresponding function at that wavelength.

To model the actual mixture of aerosols present in the Córdoba atmosphere, a linear combination of modeled irradiances using the rural (I_R) and urban profiles (I_U) was performed according to

$$I_M = C_U I_U + C_R I_R \tag{2}$$

where I_M is the irradiance calculated considering a mixture of urban and rural aerosols and C_U and C_R are the fractions of urban and rural aerosols, respectively ($C_U + C_R = 1$).

The best combination of profiles (i.e. the urban and rural percentages or C_U and C_R coefficients) was selected as the one showing the smallest difference respect to the experimental values. To find this difference we used the absolute value of the relative error expressed as a percentage:

$$relative\ error = \left(\frac{|I_M - I_E|}{I_E}\right) 100\%, \tag{3}$$

where I_E represents the experimental irradiance. The point behind partitioning the UV-B in this way is to take advantage of the default profiles provided by the model. It should be noted that, once determined that a given type of aerosols (i.e. maritime, rural, urban, continental, etc.) represents the major contributions, any model including the involved profiles could be used to build the linear combination that better reproduces the measurements.

3. Results and discussion

As it was mentioned above, two different approaches were followed to characterize and classify the collected aerosol particles and relate them with their radiative effects. They are detailed in the following subsections.

3.1. SEM-EDX

About 600 particles from 16 samples were analyzed, identifying different particles according to their chemical elements, which are shown in Table 1. From the table we can distinguish three different classes of particles, namely, carbonaceous particles (pure or in combination with other chemical elements), silicates (present as quartz, aluminum silicates and silicates mixed with Na, Fe, Ti, Ca, and Mg), and metal particles (including Fe, Mg, and Ti, all of them present as oxide particles). Relative abundance of each particle class in the samples was determined relative to the total number of particles analyzed. It should be noted that silicates occur in a small fraction compared to the carbonaceous fraction because the particles analyzed in this study correspond to PM2.5 particles. It is well known that silicates occur mostly in the coarse fraction (Viana et al., 2008).

As it was previously stated, particles were classified by following the algorithm showed in Fig. 2. Fig. 3 shows that most of the particles contain C as a main component (wt% > 60%). Among these particles only 16% are pure carbonaceous (wt% > 90%) while the rest are mixtures containing C (60% < wt% in C < 90%) and other elements. Particles with wt% of C < 60% were also found as mixtures. Note that some of these particles do not contain C. Most of these particles have Si as the main component mixed with a variable percentage of different elements. A small percentage of the particles with a wt% of C < 60% are composed mainly by Mg, Fe, Ti and O. The central pie chart shows the contribution of particles to the urban (76 ± 8)% and rural (24 ± 3)% groups. These results are in agreement with previous studies that point to mobile sources as the main sources of air particles pollution in Córdoba (López et al., 2011; Olcese & Toselli, 1998). A short description of the types of particles included in each of these groups is shown below.

3.1.1. Urban particles

They represent all the particles generated by anthropogenic activities which contribute to the air pollution in the city. Following our criteria, pure carbonaceous and mix carbon-rich particles were included in this group. The former, because they are assumed to be formed via a vaporization–condensation mechanism during combustion processes such as burning of diesel, coal, residual oil and biomass (Kittelson, 1998). The latter, because they could have been originated in combustion processes, and mixed with particles from crustal origin, construction works and traffic emissions (brake wear, tire wear and road resuspended urban dust). In more detail, the chemical differentiation of aerosols into the urban group was made based on the chemical elements found and on the previous knowledge of the site. In addition, the abundant references in the literature referring to which elements or species can be considered as tracers of the different sources was used as a guidance (Calvo et al., 2013; Viana et al., 2008, and references therein) together with the previous work on bulk chemical elements

Table 1
Number and percentage of each class of particle in the PM2.5 fraction.

Main elements (wt%)	Number of particles (597)	Percentage of the total
C	77	12.9
C/Si	89	14.9
C/Si/Al	83	13.9
C/Fe	73	12.2
C/Cr	4	0.7
C/Ba	5	0.8
C/Zn	2	0.3
C/Ni	1	0.2
C/S	6	1.0
C/Pb	2	0.3
C/Mg	13	2.2
C/Ca	54	9.0
C/Ti	2	0.3
C/Ca/Mg	35	5.9
C/Ca/S	5	0.8
Si/O	26	4.4
Si/Al	103	17.3
Si/Na	1	0.2
Si/Ti	1	0.2
Si/Fe	2	0.3
Si/Ca	6	1.0
Si/Mg	2	0.3
Mg/O	2	0.3
Fe/O	2	0.3
Ti/O	1	0.2

found in the city and the source apportionment made by López et al. (2011). For example, in Córdoba the main responsible of urban air pollution are mobile sources including diesel and gasoline powered vehicles (Olcese & Toselli, 2002) with minor contributions from industrial activities (cement and metallurgical). The four categories for the urban type were assigned considering that for diesel and gasoline power vehicles the main tracers are carbon in large abundance and minor contents of Fe, Cr, Ba, Zn, Ni, S, Pb. The occurrence of these elements is not surprising since these elements are known to be present in motor vehicle exhaust or produced through motor vehicle actions like brake wear, tire wear and road dust re-suspension (Morishita et al., 2011; Thorpe & Harrison, 2008; Viana et al., 2008). Carbon, Mg, and Ca are representative of construction activities, which were very abundant in the city, and cement plants contributions that are the main industries located within the urban perimeter and along the direction of the dominant winds (from NE).

3.1.2. Rural particles

They represent those particles originated from natural sources, and mostly include soil particles transported by the wind from the nearby rural region surrounding the city (Calvo et al., 2013; Viana et al., 2008) or resuspended soil dust. These particles contain mostly crustal elements: Si, Al, Na, Ti, Fe, Ca, and Mg. These elements appear in nature as aluminum silicates or as oxides. The major compounds in the Earth's crust consist approximately of 75% of silicates and aluminum silicates in terms of weight. Following Fig. 2 and considering that soils from Córdoba are mainly composed by aluminum silicates (e.g. Krohling, 1999), the silicon-rich particles were included in this group. The aluminum silicates are characterized by high contents of Si and Al and variable content of Na, K, Fe, S, Mg, and/or Ca. Titanium associated to these particles was also found and the same natural source was assumed for this element because it is one of the most abundant in the terrestrial core.

3.2. UV-B irradiance

In total, the UV-B irradiance for 33 days was modeled with the SBDART model. The selection of these days was based on the availability of: (1) irradiance measurements in presence of aerosols and under cloudless conditions, (2) AOD level 2.0, and (3) total ozone column data. By applying these conditions, the number of available days is significantly reduced but it assures that the aerosols are the only responsible for the observed effects on the irradiance. The data set of all selected days represents different meteorological conditions along the year. As an example, Fig. 4(a) shows the daily variation of experimental irradiance for 11 October 2000. The hourly variation of the $AOD_{340\ nm}$, as measured by AERONET, and the $AOD_{550\ nm}$, calculated from the Ångström equation, is shown in Fig. 4(b). As 340 nm is the closest wavelength to the UV-B region and 550 nm is the wavelength of the AOD required by the SBDART model, the AOD values at both wavelengths are shown. The average $AOD_{340\ nm}$ and $AOD_{550\ nm}$ values and their standard deviations were 0.29 ± 0.06 and 0.16 ± 0.02, respectively, which represent a day with a moderate loading of aerosols. Here, it is important to keep in mind that all the

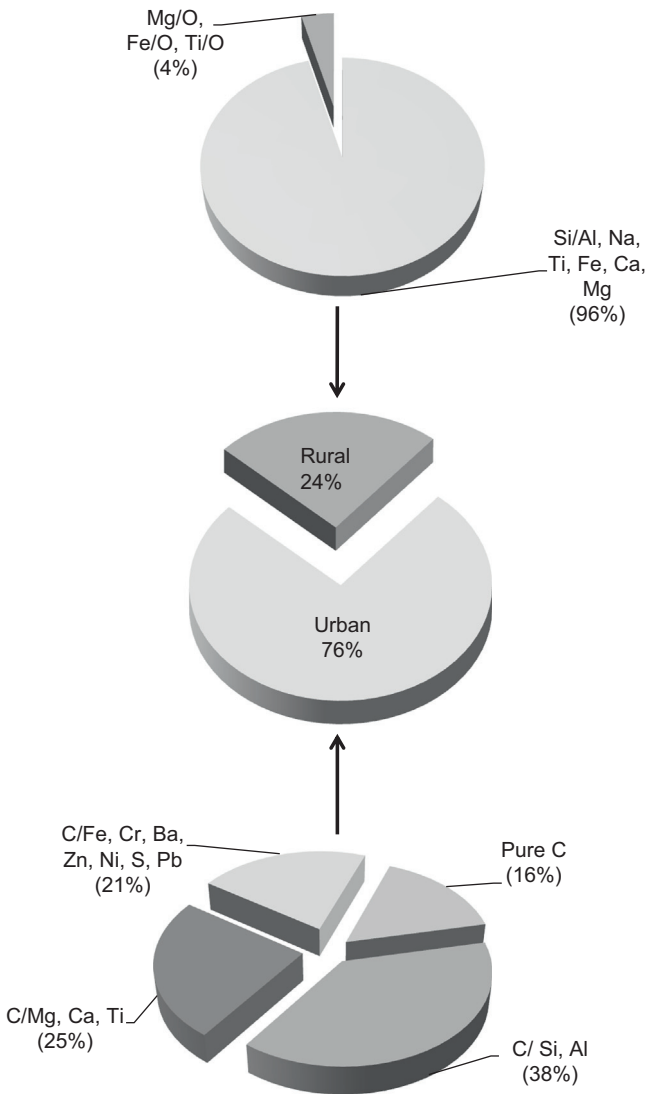

Fig. 3. Distribution of the total particles in the urban and rural groups (central pie chart), contributions to rural and urban aerosol types (upper and lower pie charts). See text for details.

calculations in this work were carried out using hourly AOD values. In Fig. 4(a). the calculated UV-B irradiance under clear-sky conditions (absence of clouds and aerosols) is shown along with the calculated irradiances including only one aerosol profile: urban or rural. Respect to the clear-sky calculations, the experimental irradiance on this day was reduced by 18%, on a daily average. The differences observed in the UV-B simulations using urban or rural profiles are due to the different optical properties considered in the two aerosol models, i.e. ω_0, g, and the Ångström coefficient (α) (see Kaskaoutis & Kambezidis, 2008). As the ω_0 value is lower in the urban model, the reduction in the corresponding irradiance is larger. It can also be observed that the experimental values lay between those calculated with only one profile, rural or urban, indicating that the results may be reproduced with a linear combination of them (Eq. (2)). Note that, for this day, the urban profile reproduces better the irradiance in the morning hours, while the rural profile does it for the afternoon hours. A possible explanation for this behavior is the presence of air masses coming from downtown during the morning hours, when the emissions of mobile sources are dominant. The relatively low level of the atmospheric boundary layer may also help to make this contribution more evident. The closeness of the experimental irradiance to the modeled one with the rural profile during the afternoon hours is also consistent with the meteorological data which showed an increase in the wind speed with wind gusts of up to 50 km h^{-1} after midday. This fact points to an increase in the contribution of the geological particles transported by the wind, reflected in the correspondence of the experimental irradiance with the one calculated with the rural profile. The ω_0 values provided by AERONET (not shown) show a marked increase in the afternoon, which is consistent with our explanation. Thus, the behavior observed in Fig. 4(a) confirms the necessity of considering the contribution of both types of aerosols. As an example, Fig. 5(a) shows the *relative error* (see Eq. (3)) as a function of C_U for different SZAs for 11 October 2000. As only urban and rural aerosols are being considered, the remaining fraction

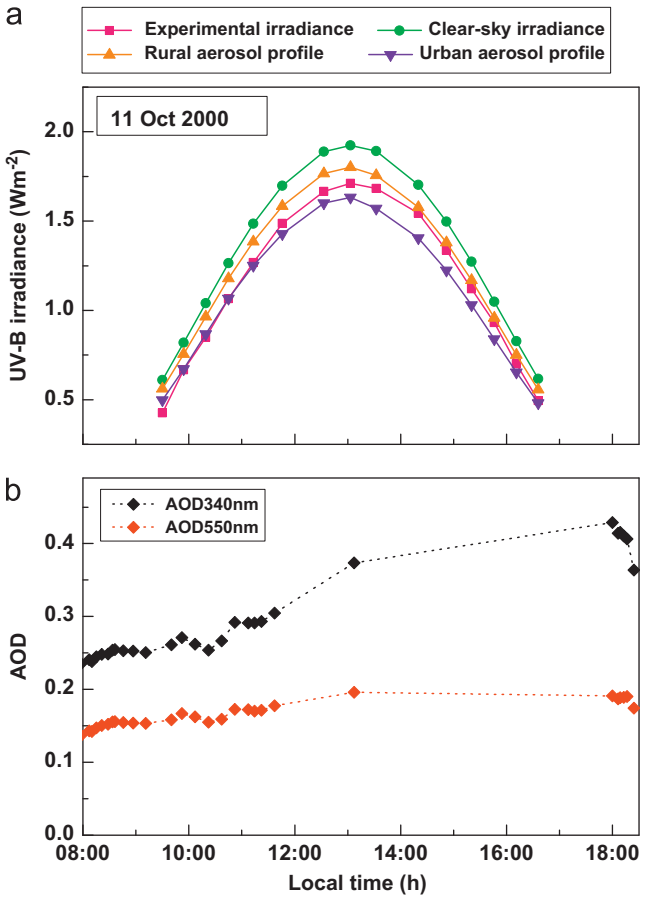

Fig. 4. (a) Hourly variation of experimental and modeled UV-B irradiances under clear-sky and aerosol loaded conditions, for 11 October 2000 (O_3=299 DU and average $AOD_{340\ nm}$=0.29). Clear-sky means absence of clouds and aerosols. (b) Daily variation of the AOD at 340 nm and 550 nm. See text for details.

corresponds to rural aerosols (C_R). As seen, the smallest relative errors are always very close to zero. It can also be seen that the C_U values which show these smallest differences vary with the SZA, ranging from 0.2 to 0.5. This result can be explained considering the changes in the AOD values and the aerosol properties along the day because of the effect of the wind, short-range transport or contributions from local sources. The best combination of profiles, on a daily average, was obtained averaging the C_U values corresponding to the smallest relative errors at each SZA. For this day, it results in 30% of urban aerosols and 70% of rural aerosols. A statistical analysis of these results is shown in Fig. 5(b), which presents the ratio (R) between modeled (urban-rural mixture) and experimental UV-B irradiance as a function of C_U. The ratio is defined as

$$R = \frac{I_M}{I_E} \tag{4}$$

Each box in Fig. 5(b) contains 50% of the R-values around the mean value for all SZAs. The mean and median values are also shown as well as the 1% and 99% percentile. This kind of graph provides additional information about the degree of dispersion of the values. From Fig. 5(b) it can be seen that the best combination of aerosol profiles, taken as a 100% in Eq. (4), is when C_U is 0.3 (30% of urban aerosols). For C_U values larger than 0.35, I_E values are underestimated while for C_U values smaller than 0.25 the opposite is true.

The same analysis was performed for the remaining 32 days selected in this work. Fig. 6 shows the results for 4 days highlighting the wide range of meteorological conditions found during the analyzed period.

Fig. 7 shows, as a box plot, the results obtained for all days with $AOD_{340\ nm}$ values >0.20. Through the analysis of this figure, it can be observed that the lowest percentage of relative error is achieved when C_U is equal to 0.7. Considering boxes laying in ± 5, a range of 0.65–0.85 is obtained. The $\pm 5\%$ was chosen based on the uncertainties involved in both, irradiance measurements and model calculations.

Fig. 8 shows $AOD_{340\ nm}$ values (Fig. 8(a)) and C_U values (Fig. 8(b)) as a function of the Julian day. Note that every point in Fig. 8(b) represents the best agreement between irradiance measurements and the irradiance obtained throughout a given linear combination of the urban and rural aerosol profiles. From the analysis of Fig. 8 it can be drawn some interesting remarks regarding the relationship between optical properties of the aerosols and the meteorology. First, Fig. 8(a) shows

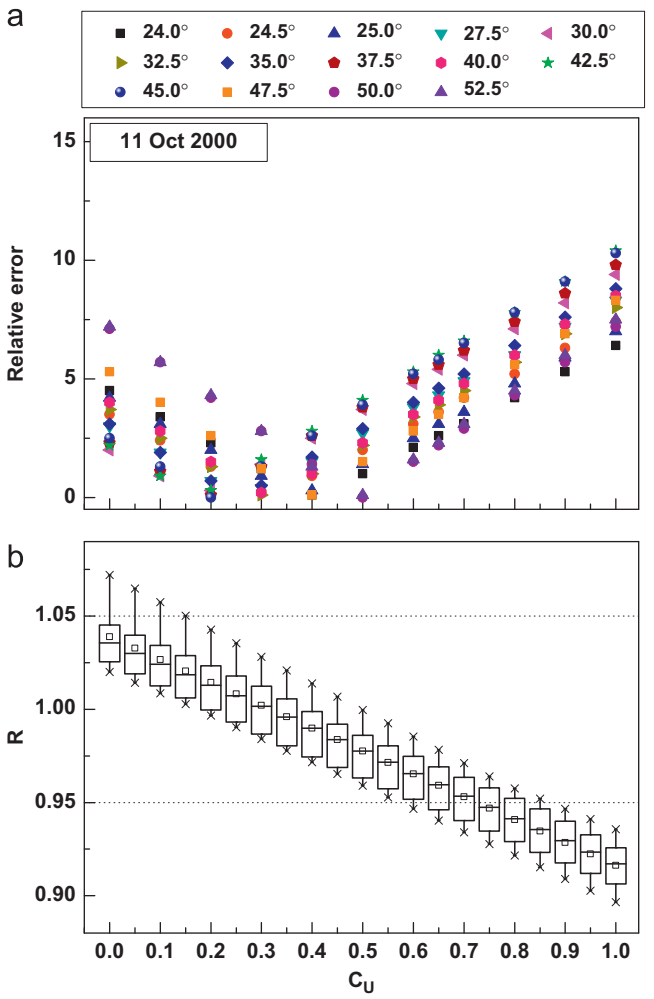

Fig. 5. (a) Relative error and (b) ratio (R) as a function of C_U values for 11 October 2000 (O_3=299 DU and average $AOD_{340\ nm}$=0.29). Numbers in the top box indicate SZA. In (b): □ represents the mean, — median, and × the 1% and 99% percentiles. See text for details.

that the $AOD_{340\ nm}$ values tend to increase during the winter–spring period, which is consistent with an increase in the C_R values (Fig. 8b). This behavior can be explained considering the meteorology of the region during this time of the year, with almost no precipitations (see Fig. 1) and strong winds prevailing from the NE direction. The low humidity, dryness of the soil, and the strong winds favor a high aerosol loading, enriched in soil particles. The opposite situation (low wind speed and frequent precipitations) is observed during summer and fall (see Fig. 1). This leads to the low AOD values observed in this period. Thus, the AOD maximum observed around September (see Fig. 8(a)) is the result of a compromise between these two counteracting meteorological factors. From Fig. 8(b) it can be seen that during this period the C_U are, in average, higher than 0.7. It could indicate that the region is mainly affected by urban sources such as emissions from traffic, urban dust and emission from industries. Thus, from Fig. 8 can be seen that meteorology plays an important role not only in the amount of aerosols but also in their composition. A second statement which confirms what it was previously mentioned is the anomalous $AOD_{340\ nm}$ value of 0.71 for the Julian Day 355 (indicated as a triangle in Fig. 8(a)). For this day the $AOD_{340\ nm}$ value is much larger than the average and correlates with an increase in the C_R values which is unexpected for this time of the year. Among the possible explanations for this anomalous $AOD_{340\ nm}$ value, we disregard the possibility of important fires in the surrounding regions. This fact was verified through the records of the National Secretary of Environment. Although some minor fires can be seen in the MODIS fire counts maps, the back trajectories calculated by using the HYSPLIT model show that the air masses arriving to Córdoba are not coming from the regions where fires were detected. Furthermore, the α value (440–870 nm) provided by AERONET for that day was 0.994, which indicates the dominance of large particles, in contraposition of what it could be expected as a result of a fire. Unfortunately, AERONET does not report other optical parameter (ω_0, g, etc.) that could shed light on this analysis. In addition to that, in that case we should have obtained higher C_U values, pointing to a higher contribution from carbonaceous particles product of biomass burning (Soto-García et al., 2011). We could not find any other explanation that could justify this anomaly, except the same meteorology which also accounts for the results for the winter-spring period.

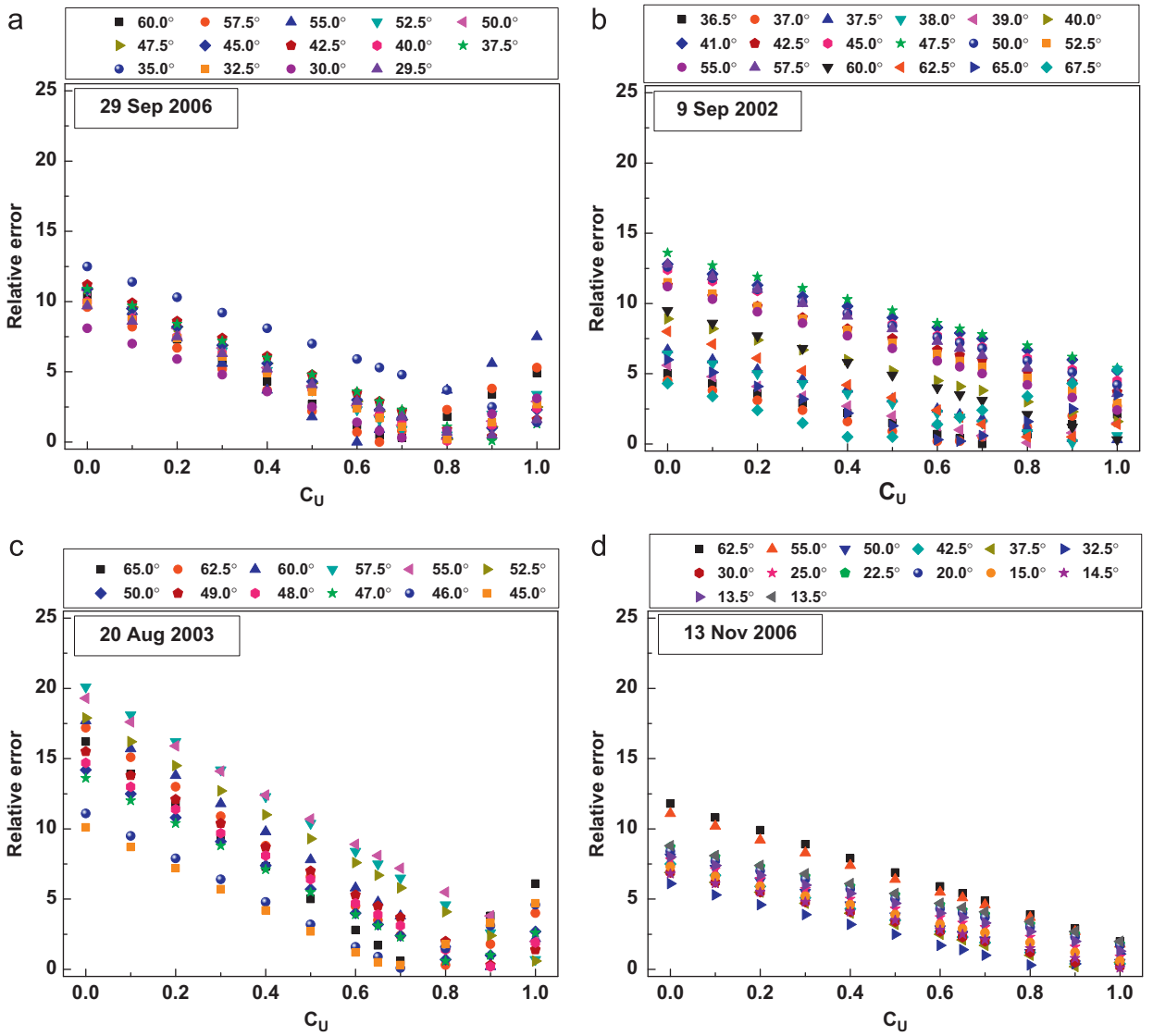

Fig. 6. Relative error as a function of C_U values for 4 selected days: (a) for 29 September 2006 (O_3=283 DU and average $AOD_{340\ nm}$=0.42), (b) for 9 September 2002 (O_3=288 DU and average $AOD_{340\ nm}$=0.23), (c) for 20 August 2003 (O_3=266 DU and average $AOD_{340\ nm}$=0.47) and (d) for 13 November 2006 (O_3=264 DU and average $AOD_{340\ nm}$=0.23). Numbers in the top box indicate SZA. See text for details.

4. Summary and concluding remarks

In this work, we used individual particle analysis and experimental UV-B irradiance measurements together with radiative transfer calculations to retrieve and compare the relative contribution of aerosol types at an urban site. To achieve that, SEM-EDX techniques were used to classify the aerosol particles collected in Córdoba City as urban or rural, resulting in a mixture of (76 ± 8)% and (24 ± 3)%, respectively. From the analysis, we found that: (1) Córdoba atmosphere contains particles composed of a wide variety of elements, (2) few particles were composed of only one pure chemical element, and (3) particles with two or more elements have variable percentages of each of them. The results of this analysis were later compared with the one obtained by calculating the UV-B irradiance for aerosol loaded days using the SBDART model. Aerosols were incorporated into the SBDART model through two of its default aerosols profiles, urban or rural, and by considering that the overall effect on surface irradiance can be reproduced by a linear combination of them. From the analysis of 33 days of irradiance measurements, we concluded that the attenuation of experimental UV-B irradiance can be modeled, in average, considering a mixture of (70 ± 7)% of urban and (30 ± 3)% of rural aerosols. The variability in the mixtures was attributed to the different meteorological conditions along the year that can affect the amounts and types (urban or rural) of the particulate matter.

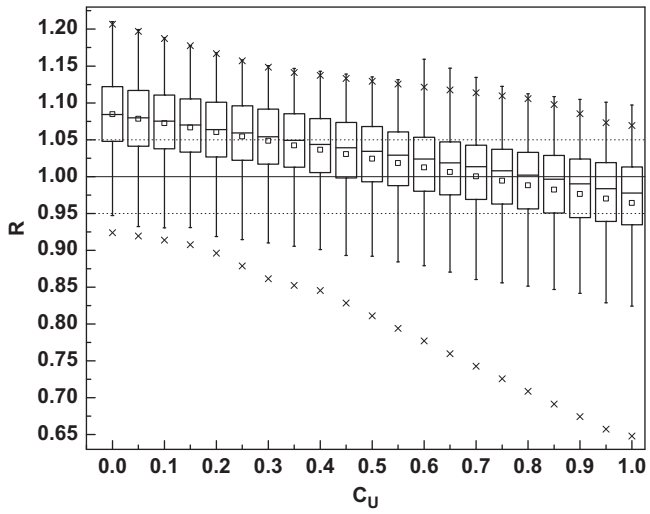

Fig. 7. Box chart showing R as a function of C_U values for all days with $AOD_{340\ nm} \geq 0.2$. Here, □ represents the mean, — median, and × the 1% and 99% percentiles.

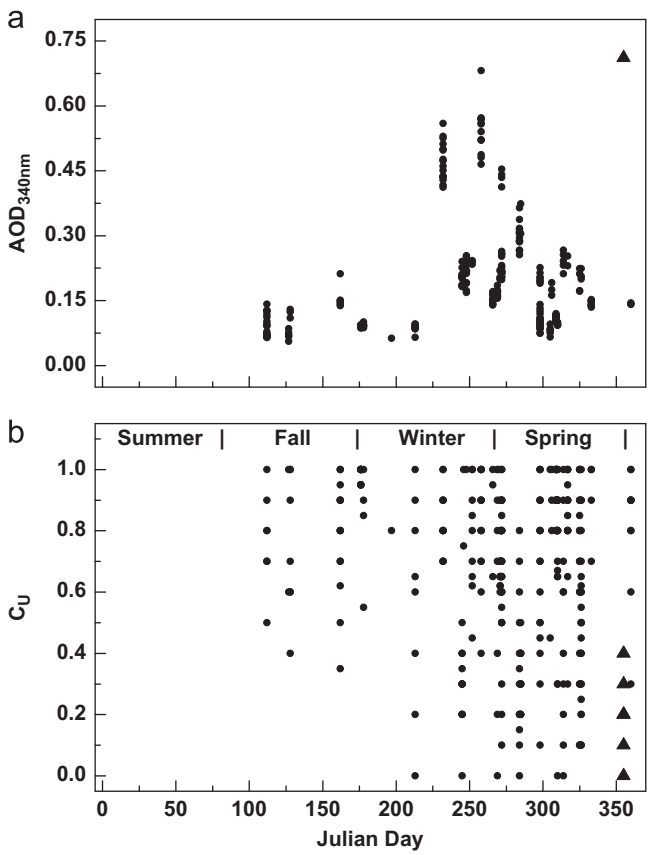

Fig. 8. (a) $AOD_{340\ nm}$ and (b) C_U values as a function of the Julian Day for all of the analyzed days (filled circles). Filled triangles represent an anomalous situation. See text for details.

For this study, we assumed that the measurements are influenced by aerosols whose chemical characteristics are similar along the whole year being the only difference the total aerosol loading. This is to say, in the average, the region receives contribution, in variable proportions, from the same types of aerosols: urban or rural. In addition, we have considered that surface properties of the aerosols in the PM2.5 fraction can be attributed to the total aerosol column. Therefore, chemical properties of the aerosols collected on the grids represent those of a well-mixed atmospheric planetary boundary layer

(Babu et al., 2002). This approach has been previously applied to correlate aerosol information retrieved from satellites with surface-level PM2.5 mass (Wang & Christopher, 2003). In a previous study of the City (López et al., 2011), it was informed that PM2.5 from Córdoba consists of a mixture of 85% urban and 15% rural aerosols. Present results are consistent and are in agreement with that study. These findings provide us with confidence about the assumptions and the approach used to correlate the relative contribution of different aerosol types with their affects on the solar irradiance at surface.

Provided the AOD and the types of aerosols are known, we showed that it is possible to determine their relative contribution just by carrying on UV-B irradiance measurements and calculations. This is to say it is possible to use the irradiance as a surrogate variable. One step forward in this direction would be to carry out concurrent SEM and irradiance measurements to explore the one to one correspondence for a long period of time. Depending on the available data, this correlation may be useful to estimate other aerosol properties (e.g. single scattering albedo of the mixture). Although we did not explore these possibilities in this work, they will be part of future works.

Taking into account the good agreement observed between the two completely different approaches used in this work we considered that a link between them is worthy to be explored. In order to do that, more particle sampling, irradiance measurements and model calculations, together with a comprehensive statistical analysis, will be required. This will certainly contribute to relate the aerosol chemical composition and their optical properties in real atmospheres.

Acknowledgments

We thank ANPCyT (Préstamo BID PICT 309), CONICET and SeCyT (UNC) for partial support of the work reported here. M.L. López and M. Achad thank CONICET and FONCYT for a Postdoctoral and Doctoral fellowship, respectively. We especially thank the PI and his staff for establishing and maintaining the Córdoba-CETT site used in this investigation. We also thank Brent Holben for permission to use the AERONET data and CONAE (Comisión Nacional de Actividades Espaciales) staff for looking after the instrument deployed in this site.

References

Aaltonen, V., Rodriguez, E., Kazadzis, S., Arola, A., Amiridis, V., Lihavainen, H., & de Leeuw, G. (2012). On the variation of aerosol properties over Finland based on the optical columnar measurements. *Atmospheric Research*, *116*, 46–55.

Andrada, G.C., Palancar, G.G., & Toselli, B.M. (2008). Using the optical properties of aerosols from the AERONET database to calculate surface solar UV-B irradiance in Córdoba, Argentina: comparison with measurements. *Atmospheric Environment*, *42*, 6011–6019.

Andreae, M.O., Schmid, O., Yang, H., Chand, D., Yu, J.Z., Zeng, L., & Zhang, Y. (2008). Optical properties and chemical composition of the atmospheric aerosol in urban Guangzhou, China. *Atmospheric Environment*, *42*, 6335–6350.

Ångström, A. (1929). On the atmospheric transmission of sun radiation and on dust in the air. *Geografiska Annaler*, *11*, 156–166.

Babu, S.S., Satheesh, S.K., & Moorthy, K.K. (2002). Aerosol radiative forcing due to enhanced black carbon at an urban site in India. *Geophysical Research Letters*, *29*(18), 1880. ⟨http://dx.doi.org/10.1029/2002GL015826⟩.

Bigelow, D.S., Slusser, J.R., Beaubien, A.F., & Gibson, J.H. (1998). The USDA ultraviolet radiation monitoring program. *Bulletin of the American Meteorology Society*, *79*, 601–615.

Bogo, H., Otero, M., Castro, P., Ozafrán, M.J., Kreiner, A., Calvo, E.J., & Negri, R.M. (2003). Study of atmospheric particulate matter in Buenos Aires city. *Atmospheric Environment*, *37*, 1135–1147.

Bond, T.C., & Bergstrom, R.W. (2006). Light absorption by carbonaceous particles: an investigative review. *Aerosol Science and Technology*, *40*, 27–67.

Calvo, A.I., Alves, C., Castro, A., Pont, V., Vicente, A.M., & Fraile, R. (2013). Research on aerosol sources and chemical composition: past, current and emerging issues. *Atmospheric Research*, *120-121*, 1–28.

Che, H., Yang, Z., Zhang, X., Zhu, C., Ma, Q., Zhou, H., & Wang, P. (2009). Study on the aerosol optical properties and their relationship with aerosol chemical compositions over three regional background stations in China. *Atmospheric Environment*, *43*, 1093–1099.

Chen, Y., Shah, N., Huggins, F., & Huffman, G. (2006). Microanalysis of ambient particles from Lexington, KY, by electron microscopy. *Atmospheric Environment*, *40*, 651–663.

de Roode, S.R., Duynkerke, P.G., Boot, W., & Van der Hage, J.C.H. (2001). Surface and tethered-balloon observations of actinic flux: Effects of arctic stratus, surface albedo, and solar zenith angle. *Journal of Geophysical Research*, *106*, 27497–27507.

Dichter, B.K., Beaubien, A.F., & Beaubien, D.J. (1993). Development and characterization of a new solar ultraviolet-B irradiance detector. *Journal of Atmospheric and Oceanic Technology*, *10*, 337–344.

Dockery, D.W. (2009). Health effects of particulate air pollution. *Annals of Epidemiology*, *19*, 257–263.

Dubovik, O., Smirnov, A., Holben, B.N., King, M.D., Kaufman, Y.J., Eck, T.F., & Slutsker, I. (2000). Accuracy assessments of aerosol optical properties retrieved from AERONET sun and sky-radiance measurements. *Journal of Geophysical Research*, *105*, 9791–9806.

Dumka, U.C., Krishna Moorthy, K., Tripathi, S.N., Hegde, P., & Sagar, R. (2011). Altitude variation of aerosol properties over the Himalayan range inferred from spatial measurements. *Journal of Atmospheric and Solar-Terrestrial Physics*, *73*, 1747–1761.

Estellés, V., Smyth, T.J., & Campanelli, M. (2012). Columnar aerosol properties in a Northeastern Atlantic site (Plymouth United Kingdom) by means of ground based skyradiometer data during years 2000-2008. *Atmospheric Environment*, *61*, 180–188.

Giles, D.M., Holben, B.N., Eck, T.F., Sinyuk, A., Smirnov, A., Slutsker, I., Dickerson, R.R., Thompson, A.M., & Schafer, J.S. (2012). An analysis of AERONET aerosol absorption properties and classifications representative of aerosol source regions. *Journal of Geophysical Research*, *117*(D17203))http://dx.doi.org/10.1029/2012JD018127.

Holben, B.N., Eck, T.F., Slutsker, I., Tanre´, D., Buis, J.P., Setzer, A., Vermote, E., Reagan, J.A., Kaufman, Y., Nakajima, T., Lavenu, F., Jankowiak, I., & Smirnov, A. (1998). AERONET – a federated instrument network and data archive for aerosol characterization. *Remote Sensing of Environment*, *66*, 1–16.

Holben, B.N., Tanré, D., Smirnov, A., Eck, T.F., Slutsker, I., Abuhassan, N., Newcomb, W.W., Schafer, J., Chatenet, B., Lavenu, F., Kaufman, Y.J., Vande Castle, J., Setzer, A., Markham, B., Clark, D., Frouin, R., Halthore, R., Karneli, A., O'Neill, N.T., Pietras, C., Pinker, R.T., Voss, K., & Zibordi, G. (2001). An emerging ground-based aerosol climatology: aerosol optical depth from AERONET. *Journal of Geophysical Research*, *106*, 12067–12097.

Hwang, H., & Ro, C.U. (2006). Single-particle characterization of "Asian dust" certified reference materials using low-Z particle electron probe X-ray microanalysis. *Spectrochimica Acta Part B*, *61*, 400–406.

Intergovernmental Panel on Climate Change (IPCC) (2007). Climate change 2007: the physical science basis. In S. Solomon, D. Qin, M. Manning, Z. Chen, M. Marquis, K.B. Avery, M. Tignor, & H.L. Miller (Eds.), *Contribution of Working Group I to the Fourth Assessment Report of the Intergovernmental Panel on Climate Change* (p. 996). Cambridge University Press: Cambridge, UK/New York, USA, p. 996.

Junkermann, W. (1994). Measurements of the J(O1D) actinic flux within and above stratiform clouds and above snow surfaces. *Geophysical Research Letters*, *21*, 793–797.
Kang, S., Hwang, H., Kang, S., Park, Y.M., Kim, H.K., & Ro, C.U. (2009). *Quantitative ED-EPMA combined with morphological information for the characterization of individual aerosol particles collected in Incheon, Korea*. *Atmospheric Environment*, 433445–3453.
Kaskaoutis, D.G., & Kambezidis, H.D. (2008). The choice of the most appropriate aerosol model in a radiative transfer code. *Solar Energy*, *82*, 1198–1208.
Kaskaoutis, D.G., Kharon, S.K., Sifakis, N., Nastos, P.T., Sharma, A.R., Badarinath, K.V.S., & Kambezidis, H.D. (2011). Satellite monitoring of the biomass-burning aerosols during the wildfires of August 2007 in Greece: climate implications. *Atmospheric Environment*, *45*, 716–726.
Kittelson, D. (1998). Engines and nanoparticles: a review. *Journal of Aerosol Science*, *29*, 575–588.
Krohling, D.M. (1999). Sedimentological maps of the typical loessic units in North Pampa, Argentina. *Quaternary International*, *62*, 49–55.
Laskin, A. (2010). Electron Beam Analysis and Microscopy of Individual Particles. In R. Signorell, & J.P. Reid (Eds.), *Fundamentals and Applications in Aerosol Spectroscopy*. CRC Press: Boca Raton, FL, pp. 463–487.
López, M.L., Palancar, G.G., & Toselli, B.M. (2012). Effects of stratocumulus, cumulus, and cirrus clouds on the UV-B diffuse to global ratio: experimental and modeling results. *Journal of Quantitative Spectroscopy & Radiative Transfer*, *113*, 461–469.
López, M.L., Ceppi, S., Palancar, G.G., Olcese, L.E., Tirao, G., & Toselli, B.M. (2011). Elemental concentration and source identification of PM10 and PM2.5 by SR-XRF in Córdoba, Argentina. *Atmospheric Environment*, *45*, 5450–5457.
Lorenzo, R., Kaegi, R., Gehrig, R., & Grobéty, B. (2006). Particle emissions of a railway line determined by detailed single particle analysis. *Atmospheric Environment*, *40*, 7831–7841.
Madronich, S., Hastie, D.R., Schiff, H.I., & Ridley, B.A. (1985). Measurements of the photodissociation coefficient of NO_2 in the atmosphere, II. Stratospheric measurements. *Journal of Atmospheric Chemistry*, *3*, 233–245.
Morishita, M., Keele, G.J., Kamal, A.S., Wagner, J.G., Harkema, J.R., & Rohr, A.C. (2011). Identification of ambient PM2.5 sources and analysis of pollution episodes in Detroit, Michigan using highly time-resolved measurements. *Atmospheric Environment*, *45*(8), 1627–1637.
Moroni, B., Cappelletti, D., Marmottini, F., Scardazza, F., Ferrero, L., & Bolzacchini, E. (2012). Integrated single particle-bulk chemical approach for the characterization of local and long range sources of particulate pollutants. *Atmospheric Environment*, *50*, 267–277.
Mugica-Álvarez, V., Figueroa-Lara, J., Romero-Romo, M., Sepúlveda-Sánchez, J., & López-Moreno, T. (2012). Concentrations and properties of airborne particles in the México City subway system. *Atmospheric Environment*, *49*, 284–293.
Olcese, L.E., & Toselli, B.M. (1997). Effects of meteorology and land use on ambient measurements of primary pollutants in Córdoba City, Argentina. *Meteorology and Atmospheric Physics*, *62*, 241–248.
Olcese, L.E., & Toselli, B.M. (1998). Statistical Analysis of PM10 Measurements in Córdoba City, Argentina. *Meteorology and Atmospheric Physics*, *66*, 123–130.
Olcese, L.E., & Toselli, B.M. (2002). Some aspects of air pollution in Córdoba, Argentina. *Atmospheric Environment*, *36*, 299–306.
Palancar, G.G., Shetter, R.E., Hall, S.R., Toselli, B.M., & Madronich, S. (2011). Ultraviolet actinic flux in clear and cloudy atmospheres: model calculations and aircraft-based measurements. *Atmospheric Chemistry and Physics*, *11*, 5457–5469, http://dx.doi.org/10.5194/acp-11-5457-2011.
Palancar, G.G., & Toselli, B.M. (2002). Erythemal ultraviolet irradiance in Córdoba, Argentina. *Atmospheric Environment*, *36*, 287–292.
Palancar, G.G., & Toselli, B.M. (2004). Effects of meteorology and tropospheric aerosols on UV-B radiation: a 4-year study. *Atmospheric Environment*, *38*, 2749–2757.
Rashki, A., Eriksson, P.G., Rautenbach, C.J.de W., Kaskaoutis, D.G., Grote, W., & Dykstra, J. (2013). Assessment of chemical and mineralogical characteristics of airborne dust in the Sistan region, Iran. *Chemosphere*, *90*, 227–236.
Ricchiazi, P., Yang, S., Gautier, C., & Sowie, D. (1998). SBDART: a research and teaching software tool for plane-parallel radiative transfer in Earth's atmosphere. *Bulletin of the American Meteorological Society*, *79*, 2101–2114.
Ro, C.U., Oh, K.Y., Kim, H., Chun, Y., Osán, J., de Hoog, J., & Van Grieken, R. (2001). Chemical speciation of individual atmospheric particles using low-Z electron probe X-ray microanalysis: characterizing “Asian Dust” deposited with rainwater in Seoul, Korea. *Atmospheric Environment*, *35*, 4995–5005.
Shettle, E.P., Fenn, R.W. (1979). Models for the Aerosols of the Lower Atmosphere and the Effects of Humidity Variations on their Optical Properties. AFGL-TR-79-0214, 94 pp. [Available from AFCRL, Hanscom Field, Bedford, MA 01731.].
Sinha, P.R., Dumka, U.C., Manchanda, R.K., Kaskaoutis, D.G., Sreenivasan, S., Moorthy, K.K., & Babu, S.S. (2013). Contrasting aerosol characteristics and radiative forcing over Hyderabad, India due to seasonal mesoscale and synoptic-scale processes. *Quarterly Journal of the Royal Meteorological Society*, *139*, 434–450.
Slezakova, K., Pires, J.C.M., Martins, F.G., Pereira, M.C., & Alvim-Ferraz, M.C. (2011). Identification of tobacco smoke components in indoor breathable particles by SEM-EDS. *Atmospheric Environment*, *45*, 863–872.
Soto-García, L.L., Andreae, M.O., Andreae, T.W., Artaxo, P., Maenhaut, W., Kirchstetter, T., Novakov, T., Chow, J.C., & Mayol-Bracero, O.L. (2011). Evaluation of the carbon content of aerosols from the burning of biomass in the Brazilian Amazon using thermal, optical and thermal-optical analysis methods. *Atmospheric Chemistry and Physics*, *11*, 4425–4444.
Srivastava, A.K., Tripathi, S.N., Dey, S., Kanawade, V.P., & Tiwari, S. (2012). Inferring aerosol types over the Indo-Gangetic Basin from ground based sunphotometer measurements. *Atmospheric Research*, *109-110*, 64–75.
Stein, A.F., & Toselli, B.M. (1996). Street level air pollution in Córdoba City, Argentina. *Atmospheric Environment*, *30*, 3491–3495.
Thorpe, A., & Harrison, R.M. (2008). Sources and properties of non-exhaust particulate matter from road traffic: a review. *Science of the Total Environment*, *400*, 270–282.
Titos, G., Foyo-Moreno, I., Lyamani, H., Querol, X., Alastuey, A., & Alados-Arboledas, L. (2012). Optical properties and chemical composition of aerosol particles at an urban location: an estimation of the aerosol mass scattering and absorption efficiencies. *Journal of Geophysical Research*, *117*, D04206, http://dx.doi.org/10.1029/2011JD016671.
Viana, M., Kuhlbusch, T.A.J., Querol, X., Alastuey, A., Harrison, R.M., Hopke, P.K., Winiwarter, W., & (…), Hitzenberger, R. (2008). Source apportionment of particulate matter in Europe: a review of methods and results. *Journal of Aerosol Science*, *39*, 827–849.
Wang, J., & Christopher, S.A. (2003). Intercomparison between satellite-derived aerosol optical thickness and PM2.5 mass: implication for air quality studies. *Geophysical Research Letters*, *30*(21), 2095.
Willis, R.D., Blanchard, F.T., Conner, T.L. (2002). *Guidelines for the Application of SEM/EDX Analytical Techniques to Particulate Matter Samples*. U.S. Environmental Protection Agency, Office of Research and Development, Research Triangle Park, N.C., EPA 600/R-02/070.